Modelling of Glass Fibre/Epoxy Composite Pipes Under Multi-Axial Loadings Using Finite Element Analysis

Z.S. Nazirah[a], M.S. Abdul Majid[a*], N.A.M. Amin[a], A.G. Gibson[b]
[a]School of Mechatronic Engineering, Universiti Malaysia Perlis, Pauh Putra Campus,
Arau, 02600, Perlis, Malaysia
[b]School of Mechanical and Systems Engineering, Newcastle University, Newcastle upon Tyne NE1 7RU, UK
*Corresponding Author: Phone. +612-736 7500, Fax. +604-9885167
Email: shukry@unimap.edu.my

***Abstract*-- The glass fibre reinforced epoxy (GRE) pipes under multi-axial loadings were studied through its performance at various temperatures and different failure criteria. Owing to the orthotropic nature of GRE pipes, it is hard to analyse the stresses generated in them. Therefore, using finite element software, an analysis was conducted to determine the first ply failure of composite pipes, which were subjected to five different stress ratios, ranging from pure hoop to pure axial loadings, at room temperature, 65 °C and 95 °C. The Tsai-Wu, Hashin and Puck failure criteria were used to predict the failure strength of composite pipes. The results were validated with experimental data obtained from previously reported studies. Subsequently, the limits associated with the axial and hoop stress were expressed by failure envelopes graph. There were differences in the results obtained for the various criteria; however, they showed relatively similar trends. During failure analysis, Hashin criterion results in superior predictions for determining the FPF of GRE pipes yielding the smallest % error between the experimental data compared to the other failure criteria. Initial failure stress found decreased at elevated temperatures, except at a 2:1 stress loading, where the initial failure stress increased.**

***Index Term*-- Finite element modelling; first ply failure; failure criteria; multiaxial stress ratio; glass/ epoxy composite pipes.**

1. INTRODUCTION

GRE pipes are being increasingly used and are becoming a crucial class of engineering material with a broad range of applications. These include high-pressure containers for chemical plants and the aerospace industry, as well as gas and liquid transfer pipes for the gas, oil and nuclear industries. This is owed to their high strength-to-weight ratio and excellent corrosion resistance [1]. The present work concerns applications in the offshore oil and gas industries, particularly composite pipelines for aqueous liquids. GRE pipes are usually designed to withstand high pressures. Their lightweight, relatively thin-walled structures facilitate handling and transportation, which results in reduced installation costs. The majority of pipes for such applications are produced by a filament winding process, and they are usually subjected to a combination of internal pressure and axial loading [2-3]. Figure 1 shows a schematic of a filament winding machine.

GRE pipes are considered to be thin-walled cylinders in which the radius-to-wall thickness ratio is greater than 10 ($\frac{r}{t} > 10$) [4]. In this research, the radius and thickness of the GRE pipes were 200 mm and 6 mm, respectively. Such GRE pipes are classified as an orthotropic material, where the material properties vary in perpendicular directions rather than the primary axes of an established coordinate system [5]. In addition, owing to their orthotropic properties, filament wound casings consisting of composite materials can be used to reduce the degree of expansion of pipes, without increasing the pipe thickness [6]. Based on previous netting analyses, this investigation focuses on the optimum winding angle of pipes, which is ±55°. In particular, previous studies have shown that an angle of ±55° is optimal for piping systems in which the applied hoop-to-axial stress loading ratio is 2:1 [7].

Fibre reinforcements are the main contributors of strength and stiffness of a composite structure. They work more efficiently when they are in bulk form because most of the fibre material becomes stronger and stiffer in this form. Common materials used to make these fibre reinforcements are a brittle material such as glass, carbon and ceramic. Composite with fibre reinforcement has excellent tensile strength and stiffness in longitudinal or fibre direction but low mechanical properties in the transverse direction and longitudinal compression strength [8].

Aziz Onder [9] proposed that mechanical behaviour can be characterised by a set of equivalent or effective module and strength properties. Lamina properties were determined by a phenomenological approach. An analytical method, finite element method and experimental method were applied to determine first failure pressure of composite pressure vessel. A glass epoxy composite layer is used and is oriented symmetrically or anti-symmetrically. The Tsai-Wu criterion is used to compute first failure pressure of composite layers.

The finite element analysis (FEA) method, originally introduced by Turner (1956), is a powerful computational technique used to obtain approximate solutions for a variety of 'real world' engineering problems that have complex domains subjected to general boundary conditions. FEA has become an

essential tool for the design or modelling of physical phenomena in various engineering disciplines [10].

Therefore, in this research, numerical analyses were performed using a finite element method (FEM) approach to evaluate the performance of thin cylindrical GRE pipes under multi-axial loadings. Xia et al. studied multi-layered filament wound composite pipes under internal pressure, and presented an exact solution [11]. Concerning the failure and composite damage of composite tubes, Ellyin and Martens experimentally investigated the biaxial fatigue behaviour of a multidirectional filament wound glass/fibre/epoxy pipe [12].

Filament wound GRE pipes have been the subject of theoretical and experimental investigations for many years. The stress–strain relationships, failure envelopes and failure mechanisms of GRE pipes under biaxial loadings have been extensively evaluated. The behaviour of GRE pipes, particularly under combinations of axial tension and internal pressure, has not been elucidated because of the scarcity of modelling data and the lack of understanding of this failure mode.

In 1998, an initiative was taken by Soden et al. to conduct a systematic study to test and compare prominent failure theories developed in the past decades. Known as the World Wide Failure Exercise (WWFE), the research was conducted by comparing the failure criteria of fibre reinforced plastics (FRP) systems subjected to biaxial stress ratios against a standard set of experimental test data, so that consistent comparison could be facilitated. Surprisingly most theories differed significantly from experimental observations even for a simple laminate analysis. It was concluded that, while there are numbers of failure criteria available, these were only successful with limited ranges of data. Some failure theories showed a wider range of applications whereas some produced predictions of greater accuracy. [13-14].

The Tsai-Wu criterion was also one of few that was highly ranked in the WWFE study [15-17] for predicting the strength of unidirectional laminates under combined loads. The approach to the WWFE was to present material properties of various laminates to participating investigators initially and have the participants predict failure

In these criteria, all stress components interact and contribute simultaneously toward the failure of the composite systems. Tsai-Hill [18] and Tsai-Wu [19] failure criteria are the two most commonly used interactive failure criteria in determining the failure of fibre reinforce polymer structures. These criteria assume linear elastic material properties and expect degradations in stiffness after the first ply failure.

However, the Puck theory is a well-known non-interactive failure criterion was rated in the WWFE study. Developed by Puck and Schűrmann [20-21], the theory is based on physical damage and failure mechanisms in the constituents. The theory takes into account the non-linear stress-strain relationship and makes allowances for a continuous and progressive decline in stiffness after the initiation of matrix cracks. This is later used to calculate the elastic constant of the lamina.

Prior to investigating the failure modes of GRE pipes subjected to a range of multiaxial load ratios, it is important that the micromechanics of GRE pipes is fully understood. Extensive work has been carried out by earlier researchers on the performance behaviour of GRE pipes [14] which is still going on. The primary concerns are the degradation of the mechanical properties of the pipes and their elastic response prior to final failure. The elastic properties of GRE pipe work are often modelled using laminate theory.

The performance of GRE pipes under multi-axial loadings will be analysed during this study. This investigation has three objectives. The first is to develop an FE model for filament wound glass fibre/epoxy composite pipes under multi-axial stress loading. The second is to simulate the effect of temperature on the GRE pipes to evaluate their performance. The final objective is to analyse and develop an FE model for GRE pipes with a winding angle of ±55° using several types of failure criteria. The material details for the GRE pipe employed in this study are presented in Table 1.

2. Experimental Methods

2.1 Model development

When a pipe is subjected to internal pressure, the stress components induced in each ply have to be measured. FEM is employed to conduct stress analysis and evaluate stress distribution in the structural layers of GRE pipes. The fibre is wound, producing a pattern, which is repeated for every two layers, until the desired laminate thickness is achieved (in this case 10 layers).

- First layer: +55° + resin
- Second layer: −55° + resin

The average wall thickness is 6 mm. The full dimensions of GRE pipes were illustrated in Figure 2.

Figure 3 shows a flowchart that details the protocol opted to predict the failure of GRE pipes during the modelling and analysis. According to the chart, all the elements of the model, including the material properties, boundary conditions and internal pressure ***P***, were established either before or during the modelling process. During the process, the failure models for the failed plies (elements) are identified, and stiffness degradation will be conducted. The structure will be evaluated to verify whether a failure has occurred. If failure does not occur, the internal pressure is increased incrementally. However, if a failure occurs, the mechanical properties are reduced using appropriate degradation rules. The obtained results are analysed and compared with experimental data. If no failure is observed, the load is further increased, and the process is repeated to perform stress analysis, as shown in Fig 3. This protocol was repeated at

elevated temperatures, and various failure criteria were considered to evaluate the performance of GRE pipes.

A progressive damage model was developed to determine the internal pressure associated with functional failure, which is a non-structural failure wherein the pipe can still sustain loading but can no longer function effectively. Structural failure, on the other hand, is expected to occur at higher pressures and temperatures; therefore, it is of vital importance to predict the functional failure strength of GRE pipes to facilitate their design. Progressive damage models are developed using four primary stages, namely model preparation, stress analysis, failure evaluation and material degradation. There will be different micro-mechanic regulations used for predicting the mechanical properties of composite layers as the output of model preparation, and the inputs for stress analysis are evaluated with respect to three different failure criteria.

ANSYS software was used during the study. Initially, engineering data associated with the properties of the materials employed in the study are set as material input to the software. These properties can be revised within the model without having to create a new project design. Figure 4 shows the properties of the materials that are employed in this research.

Figure 5 shows the entire model analysis. Many different conditions are available for selection in the ANSYS Workbench and this system was used for the static structural analysis in this study.

2.2 Finite element mesh generation

Figure 6 (a) shows a solid model of a pipe developed using the ANSYS Workbench and Fig 6 (b) displays the meshed model. Meshing is necessary to ensure that the properties are modelled accurately. Fine meshing generation would yield a more accurate and produced efficient model [22]. Analyses were performed for every meshed area, and the summation of all the areas represents the total property gradient of the model. One can control the meshing by selecting different properties for each mesh, such as the size of the meshed area, meshing style and mesh thickness. The first and most crucial step in FEA is discretisation (mesh generation). The results of the analysis depend on the type of element used. In this step, the component or part is divided into smaller divisions. In the discretisation process in this study, there were 9,595 and 1,730 nodes and elements formed, respectively. The purpose of discretisation is to perform analysis on each small division separately. In addition to these parameters, to produce reliable results with reasonable computation periods, it is important to select appropriate element types, mesh sizes and interface elements during the structural simulation.

Structural analysis is probably the most common application of the finite element method. The term *structural* (or *structure*) implies not only civil engineering structures such as bridges and buildings, but also marine, aeronautical, and mechanical structures such as ship hulls, aircraft bodies, and machine housings, as well as mechanical components such as pistons, mechanical parts, and tools [23].

2.3 Loads and boundary conditions

The GRE pipe analysis was performed using FEA. To achieve 2:1 loading, the pipe was fitted with end caps and the internal pressure was applied within the pipe. This loading condition is also known as a closed-end or pressure vessel condition. As shown in Fig. 7, the two ends of the pipe were closed and subjected to internal pressure. Two principal stresses developed: axial stress along the longitudinal direction and hoop stress along the circumferential direction.

The internal pressure loadings, ranging from pure axial to pure hoop, were estimated using the following relationships; where he hoop stress, σ_H, acting on the wall thickness is represented as

$$\sigma_H = \frac{pD}{2t} \tag{1}$$

The axial stress, σ_A, is given by

$$\sigma_A = \frac{pD}{4t} \tag{2}$$

where '*D*' is the internal diameter, *'t'* is the wall thickness, and '*p*' is the fluid pressure within the pipe. The applied pressure load was increased incrementally. Upon failure, the corresponding ply is degraded, and the resulting stress and strain distribution are calculated.

2.4 Stress analysis and failure criteria

Failure criteria are used to predict whether a layer (ply) has failed due to the applied loads. Temperature and other failure criteria can also be considered. There are numerous failure criteria available for composite material design [24]. Before the initial failure, strength analyses of fibre reinforced composite structures are significantly more complicated than those of isotropic materials. Standard failure criteria do not exist for fibre reinforced composite structural elements and thus, failure predictions are relatively unreliable.

Following the application of boundary conditions and forces, the next step is to perform structural analysis of the GRE pipe. Stress analysis is primarily carried out to determine the failure behaviour of the pressure vessel. During structural analysis, the hoop stress, axial stress and failure criteria were primarily considered. The total hoop and axial stresses in the composite pipes under multi-axial loading are shown in Figs. 8 (a-b) for 2:1 loading using the Tsai-Wu criterion. As shown in the figure, initial failure starts to occur at a pressure of 11.7 MPa and a hoop stress of 191.7 MPa.

Figure 9 illustrates the stress distribution for the composite pipe at first ply failure (FPF). Figure 10 shows the Tsai-Wu failure criterion values at FPF. This was determined to be 1.02588 for the pipe with the lay-up configuration of

[RT/±55°$_{10}$] at a stress ratio of 2:1 and an internal pressure of 11.7 MPa. The red coloured portions indicate that high stresses exist in that region, and the blue coloured portion shows the existence of little stress. The linear static analysis was performed to obtain the stress distribution in each ply. It comprised of principal stress in directions 1 and 2, as well as shear stress/strain components. The analysis is acceptable because the pipe will not experience substantial deformation, and the deflection is negligible compared with the general dimensions of the pipe.

2.5 Failure criterion

For composites, most failure criteria are considered to be macroscopic. It is important to assess the critical stress state for static or dynamic loadings. The accuracy of the failure prediction depends strongly on the criteria used. Many criteria are used to predict the failure of composite materials [25-26]. Failure theories are referred on stresses in a material axes or local axes because a lamina is orthotropic in nature. Failure theories are not based on principal normal stresses and maximum shear stresses. Failure theories are based on first, finding the stresses in the local axes and using five strength parameters of a unidirectional lamina to determine whether a lamina has failed [27].

Tsai-Wu, Puck and Hashin criteria were used to complete the objectives of this research. This approach can represent the interaction between direct and shear stresses, and can account for differences in tensile and compressive strength. The Tsai-Wu criterion is a well-known polynomial criterion [28-29]. It is the most universally used criterion, and its equation can be particularised to represent all polynomials. This approach can account for different material strengths under tensile and compressive loading. As with all polynomial criteria, it does not take into account the different mechanical behaviours of the constituents or fibre–matrix interface phenomena.

The Puck criterion is capable of predicting the risk of failure and the corresponding failure mode. It distinguishes between fibre failure and several modes of Matrix Dominated Failure (MDF), where delamination is one of these modes. The delamination strengths, typically, are estimated by slightly reducing the transverse ply strengths [30].

2.6 Degradation rules

The stress components induced in each layer are input into the failure criteria section of the programme; these stress components are determined from the stress analysis. The magnitudes of the mechanical properties are reduced, based on the failure mode, if a failure occurs in any layer [31].

3. Results and Discussion

Figure 11 shows the stress distribution of a GRE pipe at a stress ratio of 2:1 under an applied internal pressure. As the internal pressure increases, the hoop stress also increases until initial failure occurs via the employed failure criteria; the process will then cease.

Figure 12 presents a stress–strain curve at room temperature (RT) at a stress ratio of 2.1, using Tsai-Wu failure criterion. A point at which the onset of stress-strain relationship deviate from linear to become non-linear indicating a degradation in stiffness which suggests damage has already taken place. To plot the curve, the hoop stress values were determined from the results of ANSYS analysis as given in Fig. 11.

Following the validation of the developed modelling procedure, a parametric study is conducted to investigate the influence of temperature and selected types of failure criteria on the functional failure pressure. The failure envelopes for the different temperatures were compared, and the failure criteria revealed systematic trends. The effect of temperature and the selected types of failure criteria significantly influence the performance of the GRE pipes and their functional failure pressures. Moreover, an increase in temperature will also affect the mechanical properties. As shown in Table 3, the Young's modulus decreases as the temperature increases. The transverse stress component, which primarily governs the functional failure behaviour, decreases as the temperature increases while a greater stress is induced along the fibre direction.

The results in Table 4 indicate that the predicted FPF pressures are almost identical for both Puck's and Hashin's methods, namely no physical damage of the layers can be observed. However, the most appropriate failure criteria must be selected to obtain correct and accurate results. This strategy clearly shows the immediate benefit of layered composite structures, which can accommodate loading despite the occurrence of FPF. In all cases, it was observed that the primary mode of failure for FPF is matrix cracking.

The results show that the strength parameters correlate with the changes that occur in the material properties with the loading variations. The calculated values were compared with the given strength parameters, and the failure values were as expected. The failure of the composite elements leads to stress redistribution and severe stress concentration on the neighbouring composite elements. The stiffness degradation took place after the initial failure of the composite elements started. The effects of elevated temperatures significantly influence the mechanical behaviour of GRE pipes, as well as the functional failure pressures. Tables 5–7 summarise the data obtained from the analysis, which was subsequently graphically represented by the failure envelope.

The multi-axial failure envelopes for the analysis of the GRE pipes were illustrated by plotting the axial stress σ_A, against the hoop stress $\sigma_{H,}$ in the biaxial principal stress space. Figure 12 shows the initial failure stress-based failure envelopes for the GRE pipes that were analysed at RT, 65 °C and 95 °C, respectively. Each of the points denotes the initial

failure points, whereas the lines indicate the stress ratios at which the tests were conducted.

Overall, the failure envelopes generated from the FEM analysis show a high dependence on the stress ratios and test temperatures. At RT, the hoop strength (~270 MPa) was over four times greater than that of the pure axial strength (~70 MPa). This is because the load is strongly matrix dominated under pure axial loading. Therefore, as the stress ratio increases, the FEM axial and hoop stresses and experimental failure strength also increase because of the greater loads that are tolerated by, the stronger fibre.

The results showed that the optimal loading condition for a ±55° GRE pipe, regarded as the optimal design, is a hoop-to-axial stress ratio of 2:1. In the case of the FE model, the initial failure stress point was observed at a hoop stress of 193.85 MPa. However, the greatest first failure stress point for the FE model was recorded to be at a hoop stress of 338.51 MPa under a hoop-to-axial loading ratio of 4:1, although the axial failure strength was slightly lower than that obtained with the 2:1 loading. It can be observed in all the failure envelope graphs that the FE and experimental failure strengths are in close agreement with those predicted. For the 4:1 stress ratio, the axial strength starts to decrease in the hoop dominated loading region until a pure hoop loading is achieved.

Meanwhile, with the exception of the 2:1 loading condition, the initial failure stress is reduced at elevated temperatures. Highly noticeable stress reductions were observed for the pure axial and pure hoop loading conditions, where the failure mode is matrix dominated. Under pure axial loading, the initial failure stress values decreased from 70 MPa to 60.3 MPa to just 58.6 MPa at RT, 65 °C and 95 °C, respectively, which represents a reduction of almost one-third in axial strength. For the FE model, the initial failure stress associated with the hoop stress also substantially declined, with a decrease of nearly 42 % from 296.5 MPa at RT to 171.7 MPa at 95 °C. This finding is in agreement with past work by Hale, who suggested that the resin matrix softens at high temperatures, which significantly reduces its strength [32]. Under all the loading conditions, with the exception of 2:1, the stress failures are matrix dominated; therefore, this results in significantly reduced initial failure stress resistance, especially under pure hoop and pure axial loadings. At a hoop-to-axial loading ratio of 2:1, the first failure stress showed an increase on one occasion; the strength rose from 174 at RT to 201 MPa at temperatures of both 65 °C and 95 °C. This is because a loading of 2:1 is considered the optimal loading condition for a pipe with a winding angle of ±55°, where the majority of the loads are withstood by the glass fibres rather than the resin matrix.

It is believed that matrix systems become more malleable at higher temperatures. This temperature dependence results in the shrinkage of the failure envelopes where it becomes slightly narrower to accommodate the strength increase under the 2:1 loading condition. The maximum temperature is represented by the low glass transition temperature (*Tg*) of the GRE materials. When the temperature of the resin within the composite increases above *Tg*, the mechanical properties of the material degrade. This will consequently affect the interfacial bonding between the glass and fibres and reduce the efficiency of the resin to transfer the load to the fibres; hence, the mechanical properties of the material degrade. The value of *Tg* for GRE pipes is approximately 160 °C [33-34]. As the temperature reaches *Tg*, the material properties change.

With increasing temperature it is expected for material to exhibit increasing in strain to failure with time at constantly applied loads. It is widely known that many types of fibre reinforced are sensitive to temperature increase. Elevated temperatures soften the polymer matrix so that the behaviour of the composite can be significantly different from the response if the same load was applied under ambient temperatures [35-36].

A model that provides the most accurate predictions against experimental results is desired. Referring to Tables 5, 6 and 7, it can be observed that the initial failure stresses vary by the failure criteria used in the FEA; however, similar trends are produced for each failure criterion (Refer to Figure 13). From the calculated percentage error between the modelling and experimental data, the results obtained from the Hashin criterion show the lowest percentage error at RT; an error of 0.89% was obtained at a stress ratio of 2:1. This is followed by the Tsai-Wu and Puck criteria, with errors of 2.03% and 12.11%, respectively. For the stress ratio of 2:1, the lowest error percentages were recorded with the Hashin and Puck criteria at 65 °C and 95 °C, respectively. At 65 °C and 95 °C, the corresponding error percentages were 4.94% and 3.14% under the Hashin criterion, and 6.72% and 3.14% under the Puck criterion. Conversely, under the Tsai-Wu criterion, larger errors of 17.16% and 4.23% were obtained at 65 °C and 95 °C, respectively. It can be summarised that small error percentage between the Hashin and Puck criteria was observed since both were categorised under phenomenological criteria. Owing to its polynomial nature, the higher percentage error was seen under the Tsai-Wu criterion compared to those by the Hashin and Puck criteria. It can be concluded that the Hashin criterion is optimal to determine the FPF of GRE pipes. This may be because the Hashin criterion considers the effect of intermediate stress during the failure analysis, which occurs in reality. The Hashin criterion is advantageous because all the strength values can be obtained from standard material tests. Under both the Hashin and Puck criteria, failure is predicted when the matrix failure or fibre failure is equal to the unit value.

As shown in Figs. 13 various failure criteria, such as the Tsai-Wu, Puck and Hashin criteria, were programmed and implemented in the ANSYS software to determine the best performing failure criterion with the greatest accuracy for predicting the performance of GRE pipes. Figure 13 (a–c),

shows the modelled and experimental based biaxial failure envelopes for ±55° GRE pipes tested at RT, 65 °C and 95 °C. Given that the FPF point is defined as the point at which permanent damage is considered to start, it also can be referred to as the initial failure stress. In general, the failure envelopes generated from the FPF point show a strong dependence on stress ratio and test temperatures. For 2:1 test at RT, the envelope also shows that pure hoop FPF strength (~296MPa) is over four times greater than axial UEWS strength (~70MPa). This is mainly because in pure axial loading the load is strongly matrix dominated. As the stress ratio increases, the axial and hoop FPF failure strengths also increased due to the greater loads now being taken up by the stronger fibre.

For the effects of elevated temperatures, noticeable reductions were observed for the pure axial and pure hoop loading conditions, where the failure mode is matrix dominated. The failure envelope generated from FE simulated FPF correlated well with previously published experimental results [37]. Furthermore, the envelopes in Fig. 13 show that the largest decline in the pipe stiffness was found under pure axial loading, whereas less degradation was observed in pure hoop loading. For examples pipes with Tsai-Wu criterion exhibited high performances under pure axial loading whereas those with Hashin criterion showed the highest ability in the case of hoop loading at elevated temperatures. According to Hashin criteria, the longitudinal modulus reduced to zero when fibre breakage occurred. If matrix failure occurred, the transverse and shear moduli reduced to zero. The transverse stress found to increase as pressure increases, whereas reducing the longitudinal strength. The three failure criteria evaluated in this study produced comparable results concerning the performance of GRE pipes albeit difference in accuracy. Additionally, at elevated temperatures the material is an oxidising environment, which means the failure mode may become a function of the microstructure instabilities [38]. Hence for high temperatures any reliable life prediction criteria must consider the effects of multi-axially as well as that of the material microstructure. Therefore, an understanding of the failure modes and damage mechanics of structural materials under creep-fatigue loadings at elevated temperatures becomes essential for developing reliable failure criteria.

4. Conclusions

The effects of different failure criteria, such as the Tsai-Wu, Hashin and Puck criteria, on the damage initiation and failure strength of composite vessels were comparatively studied. There were differences in the results obtained for the various criteria; however, they showed relatively similar trends. During failure analysis, Hashin criterion results in superior predictions for determining the FPF of GRE pipes due to its consideration of the effect of the intermediate stress that actually occurs. Hashin's criteria yielded the smallest % error to experimental data compared to Puck and Tsai-Wu studied. Meanwhile, with the exception of the 2:1 loading condition, the initial failure stress is simulated to reduce at elevated temperatures. Highly noticeable stress reductions were observed for the pure axial and pure hoop loading conditions, where the failure mode is matrix dominated. Tsai-Wu criterion also gives good prediction at RT and 65 °C, where the functional failure stresses were recorded at 193.85 MPa and almost 200 MPa, respectively. The criterion found to closely predict the ultimate failure compared to experimental results. Overall, Hashin failure criteria give good performance to predict the damage initiation of the glass fibre/epoxy composite layers, which includes four failure modes; the fibre tension and compression, the matrix tension and compression at elevated temperatures. The finding well agrees with WWFE study which suggested the superiority of Hashin's over Tsai-Wu particularly on the failure modes identification [39].

Acknowledgements

The authors would like to thank the Ministry of Science and Technology Innovation (MOSTI), Malaysia, for its financial funding under the e-Science Fund, research grant number 03-01-15-SF0202. The authors would also like to thank the School of Mechatronic Engineering, Universiti Malaysia Perlis for providing space, lab facilities and financial assistance throughout the study.

References

[1] Bai.J, Seeleuthner.P and Bompard.P, Compos. Sci. Technol, 1997, 57 (2), 141-153.
[2] Gibson. A.G, Abdul Majid. M.S, Assaleh T.A, Fahrer. A, Rookus. C.A.P and Hekman.M, Plastic Rubber and Composites, 2011, 40(2), 80-84.
[3] Mahdi.E, Hamouda. A.M.S, Sahari B.B and Khalid Y.A, Journal of Materials Processing Technology, 2003, 132(1-3), 49-57.
[4] Griffiths. J and Gudimetla. P, Asian International Journal of Science and Technology in Production and Manufacturing, 2008, 1(2), 41-50.
[5] Nowak A.J, International Scientific Journal, 2013, 64(2), 198-204.
[6] Farooq U and Gregory K, ARPN Journal of Engineering and Applied Sciences, 2010, 5(4), 75-85.
[7] Krishnan P, Abdul Majid M.S, Afendi M, Gibson A.G and Marzuki H.F.A, Journal of Material and Design, 2015, 88,196-206.
[8] Ahmad Zaidi A.M, Abdul Hamid H, Ghazali M.I, Abdul Rahman I, Mahzan S and Yusof M.S, International Journal of Integrated Engineering, 2009, 1(1), 77-208.
[9] Bhavya S, Ravi Kumar P, Abdul Karim S.D, IOSR Journal of Mechanical and Civil Engineering 9IOSR-JMCE), 2012, 3(3), 01-07.
[10] Ananthasagaram S and Gopinath V, International Journal of Modern Engineering Research (IJMER), 2014, 2(1), 127-133.
[11] Xia M, Takayanagi H and Kemmochi K, Composite. Structure, 2001, 53(4), 483-491.
[12] Ellyin F and Martens M, Composite Science and Technology, 2001, 61(4), 491-502.
[13] Azzi, V.D. and S.W. Tsai, Experimental Mechanics, 1965, 5(9), 283-288.
[14] Abdul Majid M.S, Gibson A.G, Hekman M, Afendi M, Amin N.A.M, Plastics Rubber and Composites.2014, 43(9), 1-11.
[15] Soden, P.D., A.S. Kaddour, and M.J. Hinton, Composites Science and Technology, 2004. 64(3-4), 589-604.
[16] Hinton, M.J., P.D. Soden, and A.S. Kaddour, Strength of composite laminates under biaxial loads. Applied Composite Materials, 1996. 3(3), 151-162.
[17] Hinton. M.J, Kaddour A.S and Soden P.D. Failure Criteria in Fibre Rein-forced Polymer Composites: The World-Wide Failure Exercise, Elsevier, 2004.
[18] Azzi, V.D. and S.W. Tsai, Experimental Mechanics, 1965. 5(9), 283-288.

[19] Tsai, S.W. and E.M. Wu, A Journal of Composite Materials, 1971. 5, 58-80.
[20] Rotem, A., Prediction of laminate failure with the Rotem failure criterion. Composites Science and Technology, 1998. 58(7): p. 1083-1094.
[21] Puck, A. and H. Schurmann, Failure analysis of FRP laminates by means of physically based phenomenological models. Composite Science Technology, 1998. 58(7), 1045.
[22] Wang Y, Sun M, Zheng Z and Zhu S, International Conference on Educational and Network Technology, 2010, 6(122), 259-262.
[23] Ananthasagaram S, Gopinath V, International Journal of Modern Engineering Research (IJMER), 2011, 2(1), 127-133.
[24] Rafiee R and Amini A, Computational Material Science, 2015, 96, 579-588.
[25] Ajit K.P, IOSR Journal of Mechanical and Civil Engineering, 2013, 10(1), 47-51.
[26] Madhavi M, Rao K.V.J and Narayana Rao K, Defence Science Journal.2009, 59(1), 73-81.
[27] Shanmugavel M, Velmurugan, IOSR Journal of Mechanical and Civil Engineering (IOSR-JMCE), 11-16.
[28] Kreculj D, Rašuo B, Tehnički vjesnik, 2013, 20(3), 485-495.
[29] Tsai, S.W. and E.M. Wu, Journal of Composite Materials, 1971, (5) 58-80.
[30] Wimmer G, Schuecker C, Pettermann H.E, Wimmer et al 2006, 27-29.
[31] Laš V, Zem R, Kroupa T and Kottner R, Bull Appl. Mech, 2008, 4(14), 81-87.
[32] Blanco N, Des. Anal. Compos with Finite Element, 2010, 1-19.
[33] Bogert P, Satyanarayana A and Chunchu P, Struct.Adapt. Struct. Conf, 2006.
[34] Barrère-Tricca C, Halary J.L and Dal Maso F,Oil & Gas Science and Technology, 2002, 57(2), 169-175.
[35] Knox E.M, Cowling M.J and Hashim S.A, Composites: Part A, 2000, 31, 583-590.
[36] Vijayaraghavan G.K and Sundaravalli S, Flash Thermography, 2005, 52(9), 481-487.
[37] Abdul Majid M.S, Assaleh T.A, Gibson. A.G, Hale J.M, Fahrer A, Rookus C.A.P and Hekman M, Compos. Part A Appl. Sci. Manuf, 2011, 42(10), 1500-1508.
[38] Ming. D, Robert J.A study of failure prediction and design criteria for fiber composites under fire degradation, Composites Applied science and Manufacturing, 1999, 30, 123-131.
[39] Hashin Z. Failure criteria for unidirectional fiber composites, J Appl Mech, 1980, 47.329-334.

List of Figures

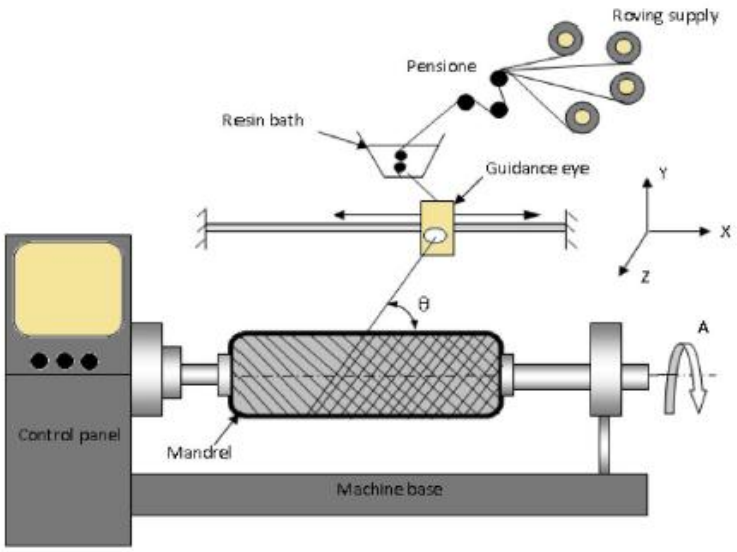

Fig. 1. Schematic of the filament winding process [3].

L = 2000 mm t = 0.6 mm
D = 206 mm Θ = ± 55
d = 200 mm n = 10 layers

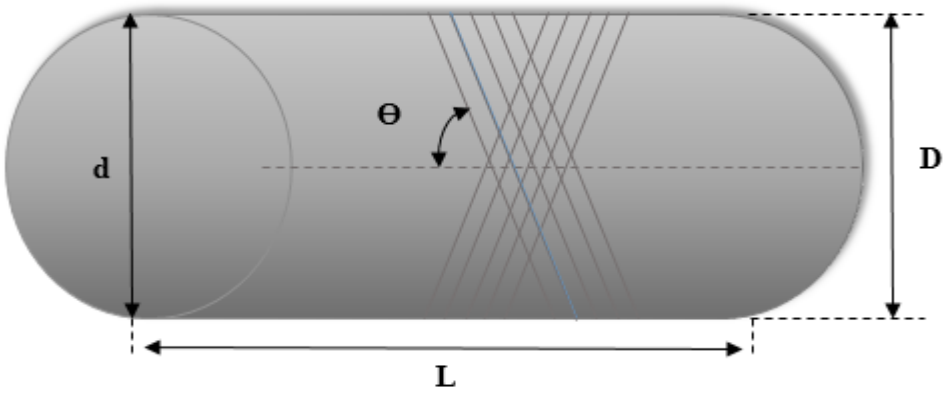

Fig. 2. Dimensional characteristics of pipe modelling

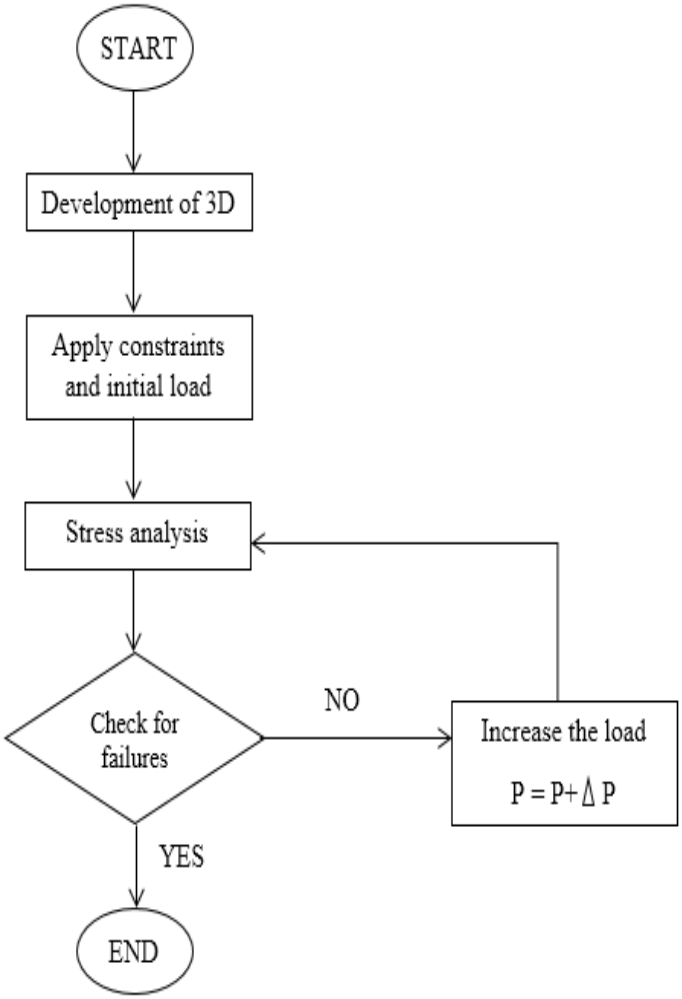

Fig. 3. Flow chart for failure prediction modelling of composite laminates.

Properties of Outline Row 3: GRE

	A	B	C
1	Property	Value	Unit
2	Density	2000	kg m^-3
3	Orthotropic Elasticity		
4	Young's Modulus X direction	44920	MPa
5	Young's Modulus Y direction	11406	MPa
6	Young's Modulus Z direction	11406	MPa
7	Poisson's Ratio XY	0.28	
8	Poisson's Ratio YZ	0.071	
9	Poisson's Ratio XZ	0.28	
10	Shear Modulus XY	4603	MPa
11	Shear Modulus YZ	3846.2	MPa
12	Shear Modulus XZ	4603	MPa

Fig. 4. Engineering data used for GRE pipe model.

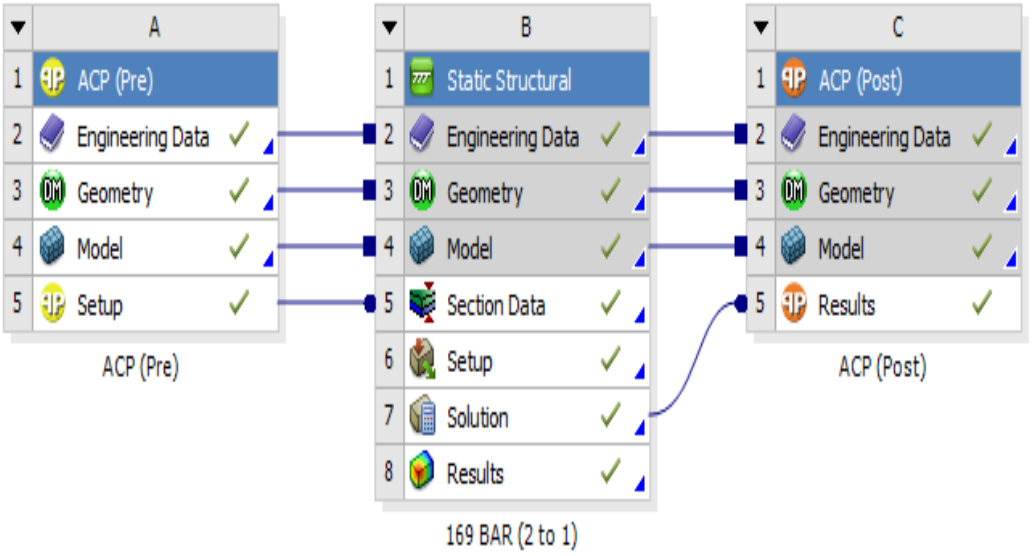

Fig. 5. Composite pipe analysis of the model

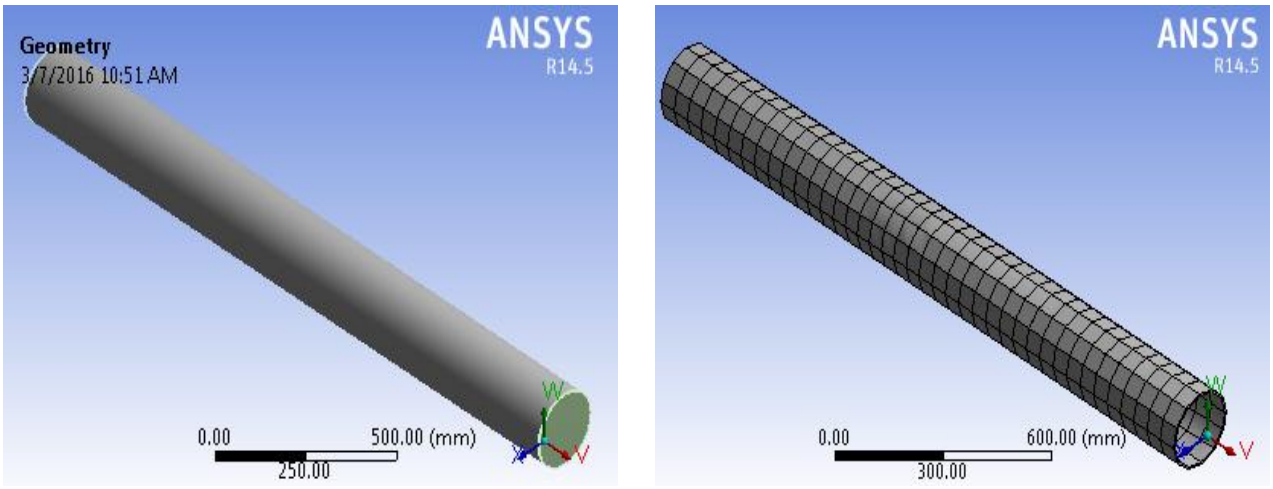

(a) (b)

Fig. 6. Model development using ANSYS software; (a) solid model of GRE pipes; (b) meshed model of GRE pipes.

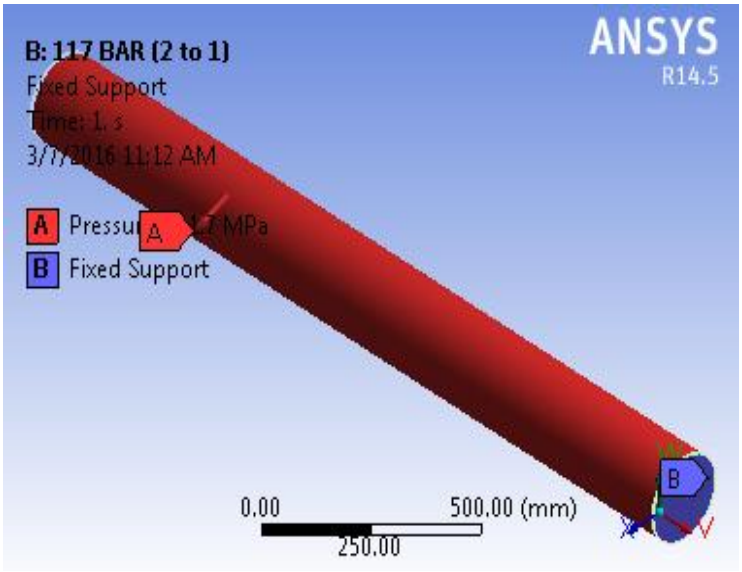

Fig. 7. The load and boundary conditions applied for the GRE pipe analysis.

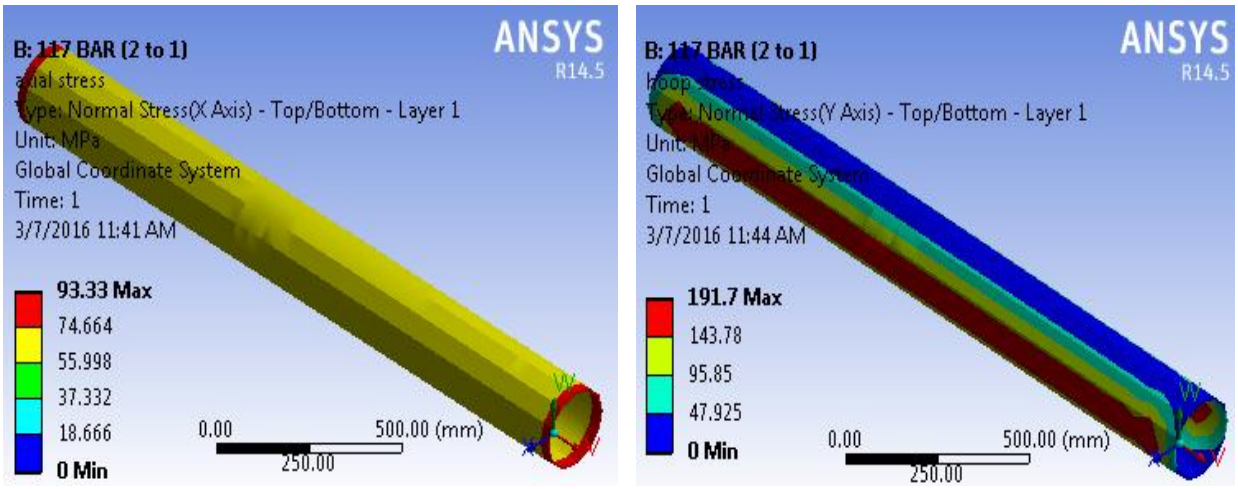

(a) (b)

Fig. 8. Structural analysis. (a) axial stress; (b) hoop stress at a stress ratio of 2:1 using Tsai-Wu criterion.

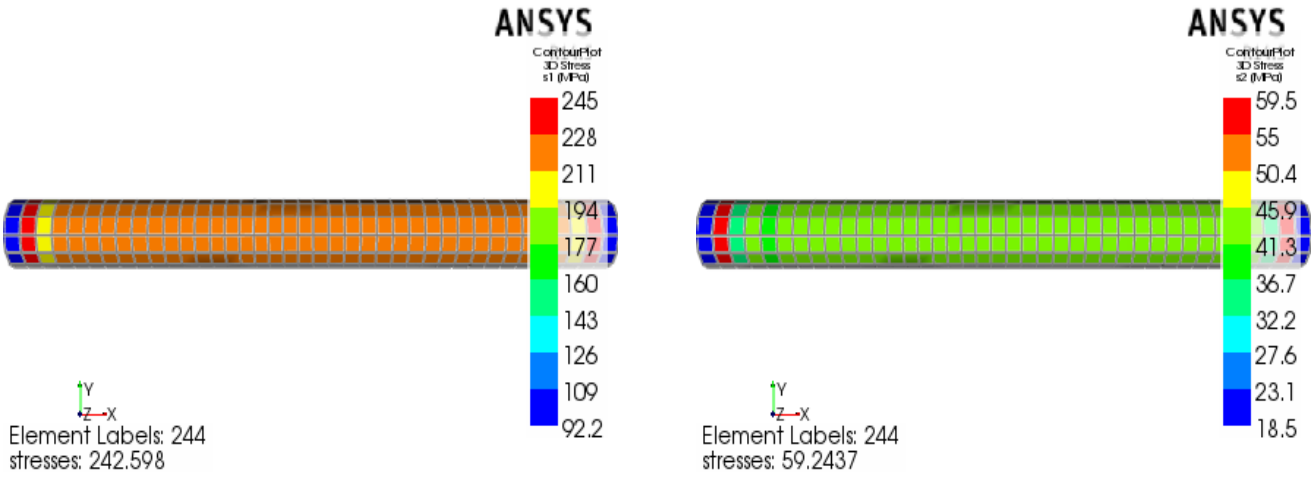

(a) (b)

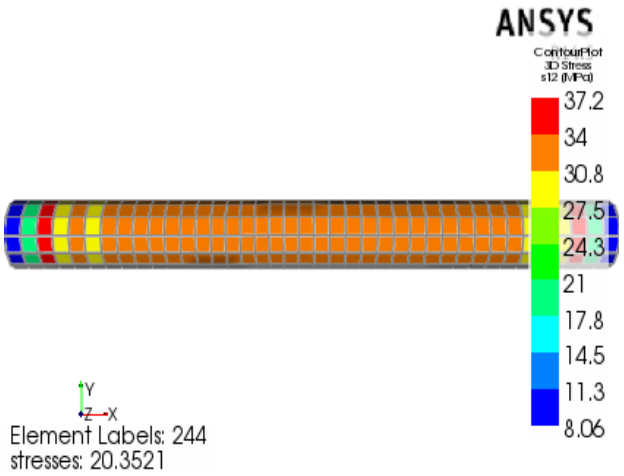

(c)

Fig. 9. Stress deformation: (a) principal stress in direction 1 (s1), (b) principal stress in direction 2 (s2), (c) in-plane shear stress (s12) at a 2:1 stress ratio using Tsai-Wu criterion.

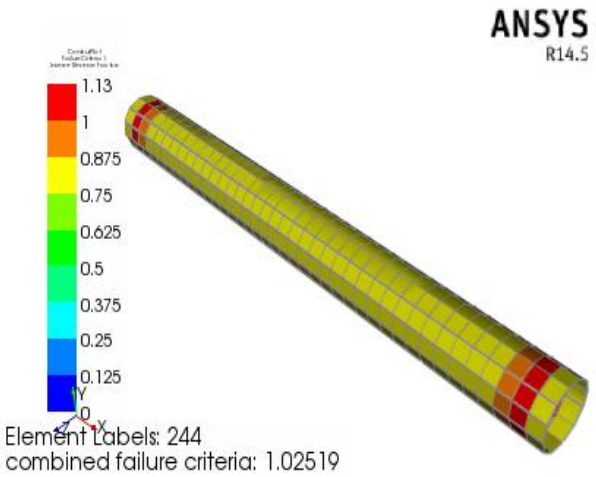

Fig. 10. Failure distribution at maximum load for a stress ratio of 2:1 using Tsai-Wu failure criterion.

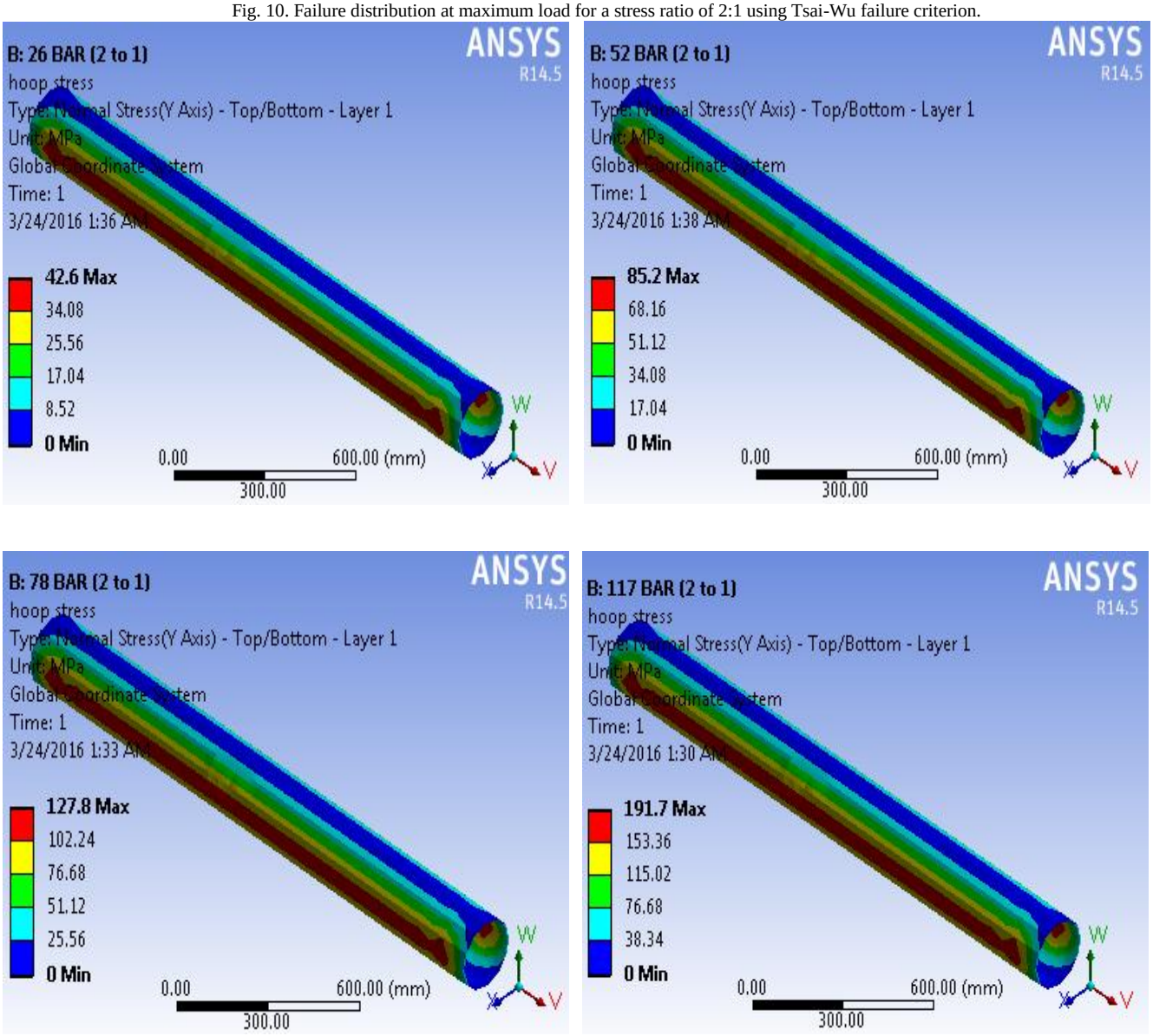

Fig. 11. Stress distribution of GRE pipe at a stress ratio of 2:1.

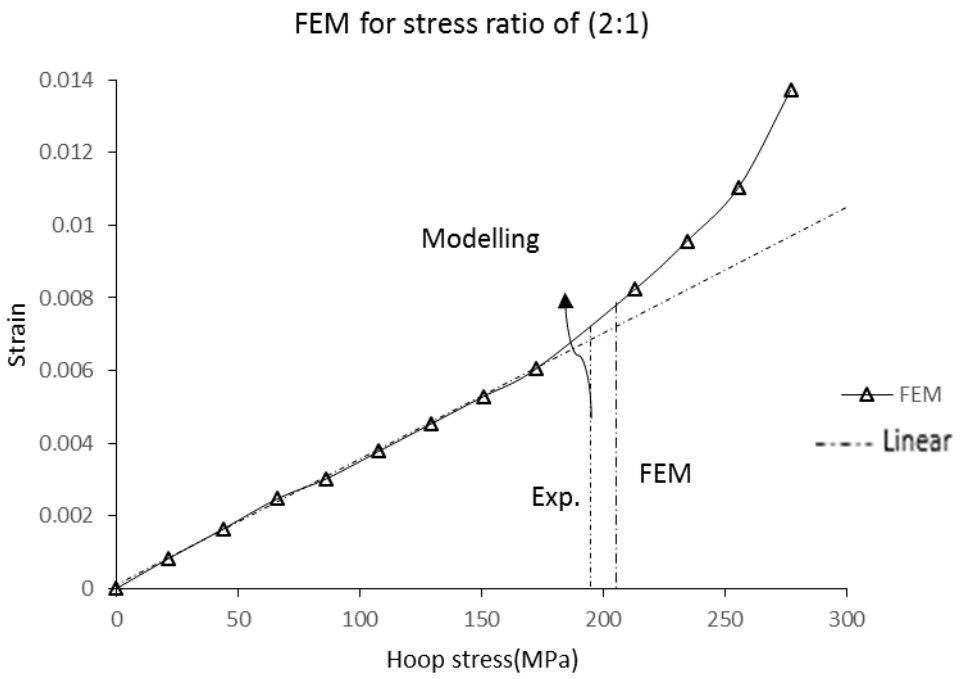

Fig. 12. Stress–strain curve at a stress ratio of 2:1 at room temperature.

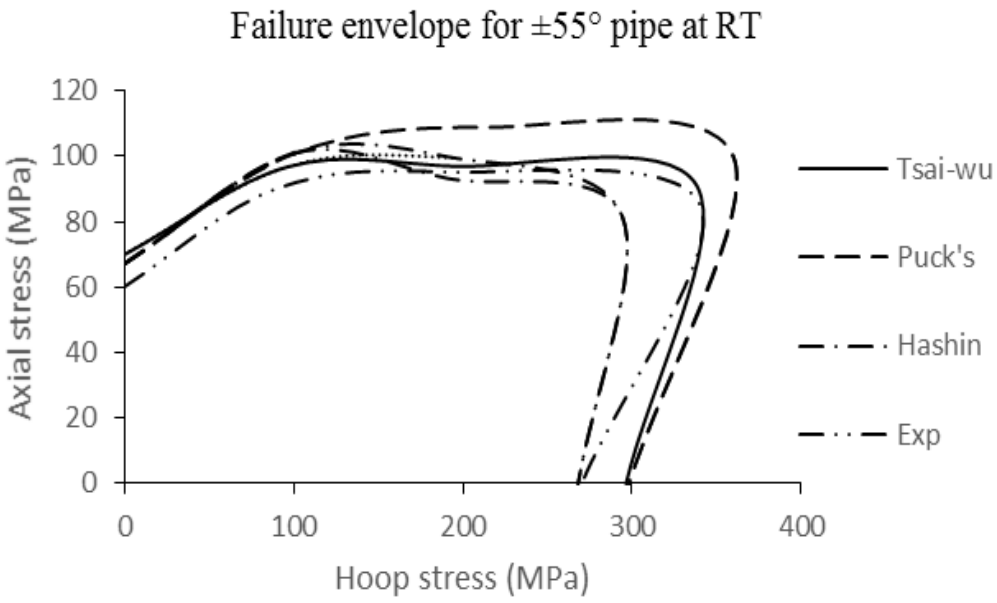

(a)

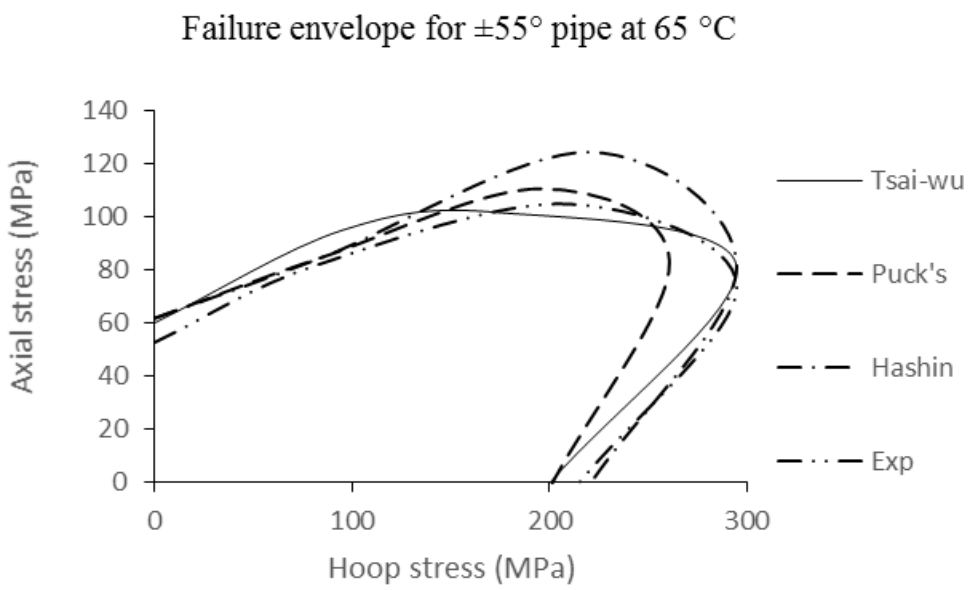

(b)

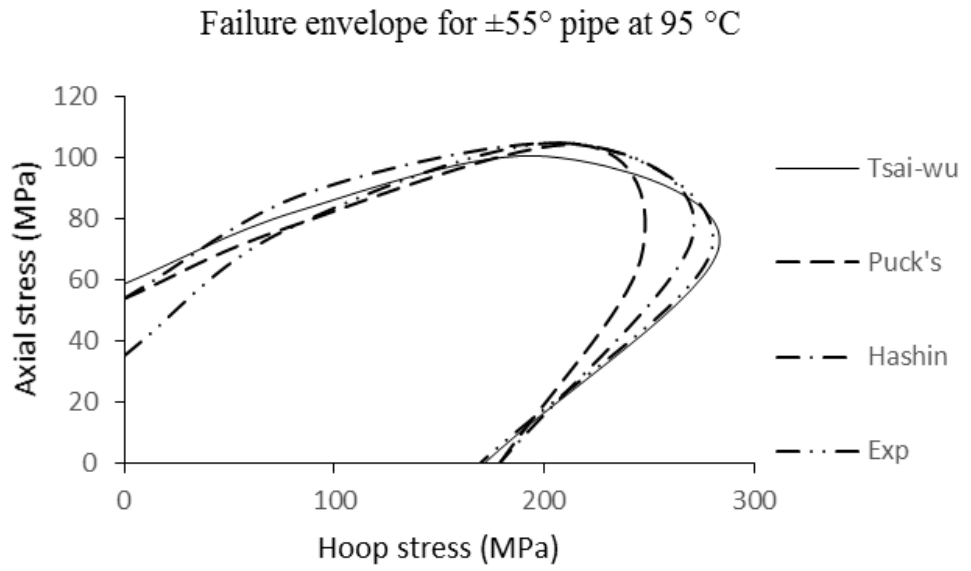

(c)

Fig. 13. Combination of failure criteria in failure envelope for GRE pipe at (a) RT, (b) 65 °C and (c) 95 °C.

List of Tables

Table I
Material description [14].

Title	Description
Fibre	E-Glass
Type of fibres	Long and continuous
Type of composite	Laminate
Matrix	Epoxy
Orientation	±55°
No. of ply	10

Table II
Mechanical property of E-glass fibre and Epoxy resin [14]

Property		E-glass	Epoxy resin
Elastic modulus	E (MPa)	73000	2800
Shear modulus	G (MPa)	30400	1000
Poisson's ratio	v (-)	0.2	0.4
Density	ρ kgm^{-3}	2600	1200

Table III
Physical and mechanical properties of GRE pipes at various temperatures [14].

Physical and mechanical properties	25 °C (RT)	65 °C	95 °C
Internal diameter (mm)	200	200	200
Average wall thickness (mm)	6	6	6
Length of pipes (mm)	2,000	2,000	2,000
No. of ply	10	10	10
Density, ρ kgm^{-3}	2,000	2,000	2,000
Matrix Young's modulus E_m, MPa	2,800	2,240	1,680
Fibre Young's modulus E_g, MPa	73,000	58,400	43,800
Axial Young's modulus E_a, MPa	11,700	9,000	7,000
Hoop Young's modulus E_h, MPa	20,500	16,300	12,000
Ply stiffness, fibre direction E_1, MPa	44,900	36,000	27,000
Ply stiffness, transverse fibre direction E_2, MPa	11,400	9,100	6,800
Poison's ratio, v_{12}	0.28	0.28	0.28
Poison's ratio v_{21}	0.071	0.071	0.071
Shear modulus G_{12}, MPa	4,600	3,600	2,800

Table IV
Predicted pressure for first ply failure (FPF) using Tsai-Wu, Puck and Hashin failure criteria at a stress ratio of 2:1

Temperature (°C)	FPF Pressure (MPa)		
	Tsai-Wu	Puck	Hashin
RT	10.4	9.1	10.4
65	10.5	7.5	7.5
95	10.4	6	6

Table V
Failure envelop for a pipe with a winding angle of ±55° using the Tsai-Wu failure criterion; (a) RT; (b) 65 °C; (c) 95 °C.

Stress Ratio	Experimental			Tsai-Wu					
	RT σhp (MPa)	65°C σhp (MPa)	95°C σhp (MPa)	RT σhp (MPa)	% Error	65°C σhp (MPa)	% Error	95°C σhp (MPa)	% Error
0:1	60(axial stress)	53(axial stress)	35(axial stress)	70(axial stress)	17	60(axial stress)	14	59(axial stress)	67
1:1	90	82	76	97	8	95	16	82	8
2:1	190	210	210	194	2	174	17	201	4
4:1	340	295	280	339	0	294	0	283	1
1:0	270	215	170	297	10	200	7	172	1

Table VI
Failure envelop for a pipe with a winding angle of ±55° using the Puck failure criterion; (a) RT; (b) 65 °C; (c) 95 °C.

Stress Ratio	Experimental			Puck's					
	RT σhp (MPa)	65°C σhp (MPa)	95°C σhp (MPa)	RT σhp (MPa)	% Error	65°C σhp (MPa)	% Error	95°C σhp (MPa)	% Error
0:1	60(axial stress)	53(axial stress)	35(axial stress)	67(axial stress)	12	62(axial stress)	17	54(axial stress)	54
1:1	90	82	76	101	12	85	3	77	1
2:1	190	210	210	213	12	196	7	217	3
4:1	340	295	280	360	6	293	1	271	3
1:0	270	215	170	298	10	201	6	179	5

Table VII
Failure envelop for a pipe with a winding angle of ±55° using the Hashin failure criterion; (a) RT; (b) 65 °C; (c) 95 °C.

Stress Ratio	Experimental			Hashin					
	RT σhp (MPa)	65°C σhp (MPa)	95°C σhp (MPa)	RT σhp (MPa)	% Error	65°C σhp (MPa)	% Error	95°C σhp (MPa)	% Error
0:1	60(axial stress)	53(axial stress)	35(axial stress)	67(axial stress)	12	62(axial stress)	16.77	54(axial stress)	54
1:1	90	82	76	101	12	85	3.35	89	17
2:1	190	210	210	192	1	220	4.94	217	3
4:1	340	295	280	294	13	295	0.05	271	3
1:0	270	215	170	269	1	221	2.70	179	5